Nucleobase Pair Analogues 2-Pyridone·Uracil, 2-Pyridone·Thymine, and 2-Pyridone·5-Fluorouracil: Hydrogen-Bond Strengths and Intermolecular Vibrations

Andreas Müller and Samuel Leutwyler*

Departement für Chemie und Biochemie, Universität Bern, Freiestrasse 3, CH-3012 Bern, Switzerland

Received: March 3, 2004; In Final Form: April 30, 2004

Due to the ultrafast nonradiative decay of the uracil (U), thymine (T), and 5-fluorouracil (5-FU) nucleobases, resolved vibronic spectra of nucleobase dimers with U, T, or 5-FU chromophores have not yet been observed in the gas phase. 2-Pyridone (2PY) is a fluorescent hydrogen-bonding analogue of U with a single N−H donor and C═O acceptor group. We report the mass-selected $S_1 \leftarrow S_0$ vibronic spectra of 2PY·U, 2PY·T, and 2PY·5-FU, revealing properties of their H-bonds free of stacking interactions and backbone constraints. The in-plane H-bond vibrations, ω', χ', σ', are observed for all three dimers; the out-of-plane vibrations β', τ' and the overtone of the stagger mode $2\delta'$ are measured for 2PY·T and 2PY·U. The experimental frequencies are in good agreement with the ab initio calculated frequencies of the most stable H-bonded isomer, which involves the N1−H and C2═O groups of U, T, or 5-FU as H donor/acceptor. The H-bond dissociation energies follow the sequence T ≈ U < 5-FU. However, the experimental S_1 state H-bond stretching force constants increase in the sequence U < T < 5-FU. The absence of fluorescence from these dimers implies that the S_1 lifetimes of 2PY in these complexes are >20 times shorter than those in the other 2PY·X complexes measured so far. Energy transfer from 2PY to U (T, 5-FU) is suggested as the cause, which implies that the $n\pi^*$ S_1 states of U, T, and 5-FU, which have never been directly observed, lie below the S_1 $\pi\pi^*$ state of 2PY.

1. Introduction

The low-frequency dynamics and collective vibrational modes of DNA have been extensively studied because of their relevance for biological processes, using techniques such as neutron scattering, NMR, and Raman spectroscopy.[1−3] However, the hydrogen-bond vibrational frequencies between the base pairs are strongly influenced by steric and energetic constraints imposed by the DNA backbone and by interactions with nearby solvent molecules and ions. The transitions are often masked by collective modes of the DNA backbone, and assignments are often difficult.[4,5] To probe and understand the hydrogen bond and other pair interactions of the nucleobases, it is necessary to remove them from their biological environment and study them in the gas phase.[6−16] The biological relevance of doubly hydrogen-bonded U·U "wobble" dimers is well established from crystal structures of RNA oligomers,[17−20] ribozymes,[21] and ribosomal RNA subunits.[22] 5-Fluorouracil (5-FU), which has nearly the same size and shape as uracil, irreversibly inhibits the transition state of thymidylate synthase, which catalyzes the methylation of deoxyuridylate (dUMP) to deoxythymidylate (dTMP).[23] Due to its powerful and specific "suicide substrate" mechanism,[24] 5-FU is in wide clinical use as a chemotherapeutic antitumor agent.

The spectra of uracil (U) and thymine (T, 5-methyluracil) in supersonic jets are broad, with onsets at 36 600 cm^{-1} for U and 36 300 cm^{-1} for T.[25] Due to their ultrarapid nonradiative decay,[26,27] resolved vibronic spectra of nucleobase dimers with U, T, or 5-FU as chromophores have not been observed so far in the gas phase. To circumvent these photophysical limitations, we employ a nucleobase analogue that exhibits narrow-band absorption and emission spectra in supersonic jets: the 2-pyridone (2PY) molecule, shown in Figure 1, is analogous to U, T, and 5-FU, exhibiting the same N−H donor and C═O acceptor groups. The 2-pyridone dimer, (2PY)$_2$, has antiparallel N−H···O═C hydrogen bonds with a H-bonding topology analogous to that of the uracil wobble dimer U·U.[17,18] Its symmetric doubly hydrogen-bonded structure,[28,29] intermolecular vibrations,[30] and ultrafast excited-state energy transfer[31] have been studied. The perfect fit of the two H-bonding contacts in (2PY)$_2$ leads to a very high double H-bond energy of ~20 kcal/mol and a high propensity for gas-phase dimerization.[32]

Isolated guanine·cytosine (G·C), G·G, and adenine·thymine (A·T) dimers have been investigated in supersonic jets using resonant two-photon ionization, IR−UV, and UV−UV hole-burning methods.[8,11,14] For G·C, the analysis of the N−H and O−H stretching vibrations shows that the observed dimer is in the Watson−Crick configuration, but with cytosine in its enol form. For A·T, the Watson−Crick base pair is not the most stable isomer, and its calculated vibrational spectrum is not in agreement with the observed spectrum.[14]

Here, we investigate the mixed dimers 2PY·U, 2PY·T, and 2PY·5-FU, in which 2PY acts as the UV chromophore, avoiding the photophysical drawbacks of U, T, and 5-FU noted above. While gas-phase U·U and T·T can exist in eight H-bonded forms, as shown by theoretical investigations,[33] 2-pyridone forms only two H-bonds, which restricts the number of isomers to only three. The comparison of the spectra of 2PY·U, 2PY·T, and 2PY·5-FU allows one to determine the effects of methylation and fluorination on the ground- and excited-state binding energies, vibrational frequencies, and intermolecular forces.

2. Theoretical Methods and Results

2.1. Isomers, Structures, and Binding Energies. As shown in a number of theoretical studies, U can exist in 13 different

---

* Corresponding author. E-mail: leutwyler@iac.unibe.ch.

10.1021/jp049033h CCC: $27.50 © 2004 American Chemical Society
Published on Web 06/23/2004

TABLE 1: 2-Pyridone·Uracil, 2-Pyridone·Thymine, and 2-Pyridone·5-Fluorouracil Calculated PW91/6-311++G(d,p) Ground-State Binding Energies D_e, Dissociation Energies D_0, Basis Set Superposition Errors BSSE, Excited-State Dissociation Energies $D_0(S_1)$, and Barriers to Pyramidalization in the S_1 State (in kcal/mol)

isomer	U1	U2	U3	T1	T2	T3	F1	F2	F3
D_e	−20.7	−16.7	−15.3	−20.5	−16.4	−15.5	−21.2	−17.0	−16.1
D_0	−19.8	−15.8	−14.6	−19.6	−15.7	−14.8	−20.3	−16.4	−15.4
BSSE	0.9	0.9	0.9	0.9	0.9	0.9	0.8	1.0	1.0
$D_0(S_1)^a$	−16.7			−16.6			−17.0		
barrier	0.040	0.025	0.040	0.034	0.031	0.026	0.050	0.047	0.051

[a] From $D_0(S_0)$ and the experimental blue-shift of the 0^0_0 transition.

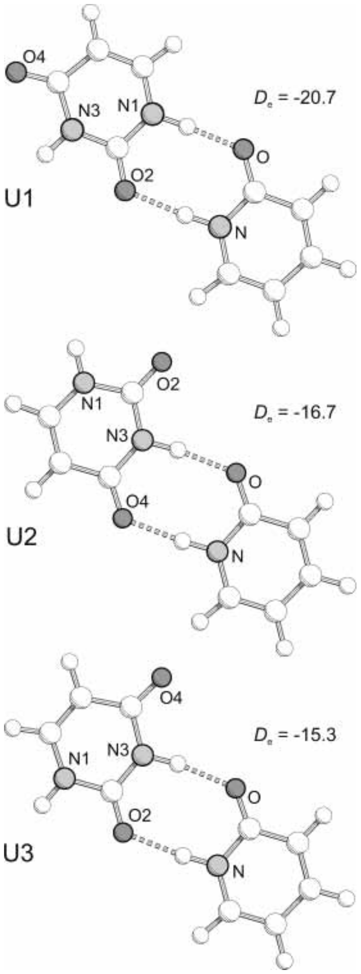

Figure 1. Minimum energy structures of three isomers of 2-pyridone·uracil (2PY·U) calculated at the PW91/6-311++G(d,p) level. Binding energies D_e are in kcal/mol.

tautomeric and rotameric forms.[34−40] With all ab initio theoretical methods, the energy gap between the most stable 2,4-diketo tautomer of U and the next higher keto−enol tautomer is calculated to be 10−12 kcal/mol. Only the 2,4-diketo tautomer has been identified experimentally in solution and in the gas phase, and we consider only this tautomer.

We performed calculations for the S_0 and S_1 states. The ground-state structures, binding energies D_e, dissociation energies D_0, and harmonic vibrational frequencies were calculated using the B3LYP and PW91 density functionals and the 6-311++G(d,p) basis set. All structure optimizations were unrestricted and converged to planar (C_s symmetric) geometries. The D_e and D_0 values are compiled in Table 1, which also gives the basis set superposition errors (BSSE).[41−43] For the analogous dimer $(2PY)_2$, we have shown that the PW91/6-311++G(d,p) method yields structural and binding energy properties which are in excellent agreement with those obtained by MP2 complete basis set extrapolations.[32] The most stable isomers involve two antiparallel N−H···O═C hydrogen bonds. Several other coplanar isomers with C−H···O═C hydrogen bonds were also optimized and are found to be 5−10 kcal/mol less stable.[44] The "stacked" complexes are expected to be 8−10 kcal/mol less stable, judging by the recent high-level calculations by Leininger et al. on stacked U·U dimers.[45]

The three N−H···O═C H-bonded isomers of 2PY·U are shown in Figure 1. Isomer U1 is H-bonded via the N1−H and C2═O groups, also called the "sugar edge".[46] With $D_e = -20.7$ kcal/mol, it is by far the most stable isomer. Maintaining the C2═O acceptor group of uracil and exchanging the N1−H by N3−H reduces D_e by 5.4 kcal/mol or 25%, resulting in the least stable isomer U3, cf. Figure 1. Exchanging the C2═O acceptor by C4═O and keeping the N3−H donor yields the isomer U2 which is 1 kcal/mol more stable than U3. The U2 and U3 isomers are Watson−Crick-type dimers, and both have been observed in rRNA,[22] RNA oligomers,[20] and ribozyme[21] crystal structures.

For 2PY·T, the three analogous isomers are denoted T1−T3. They exhibit the same energetic ordering as the 2PY·U isomers, as shown in Table 1. Depending on the isomer, the methylation slightly decreases or increases the binding energy D_e, but only by about 1%: isomer T1 is 0.2 kcal/mol less stable than U1 and T2 by 0.3 kcal less than U2. However, the isomer T3 is 0.2 kcal/mol more stable than U3. The analogous F1−F3 isomers of 2PY·5-FU follow the same sequence of H-bond binding energy. Fluorination at the 5-position increases the D_e by about 2−5%, depending on the isomer.

The finding that the three most stable structures involve the N1−H donor site of uracil are in agreement with previous B3LYP density functional calculations of the gas-phase deprotonation energies of uracil, thymine, and 5-fluorouracil: for all three species, the N1−H site is 10−14 kcal/mol more acidic than the N3−H.[47−50] Furthermore, the measured gas-phase acidity of uracil $\Delta H_{acid}^\circ = 333 \pm 4$ kcal/mol is in excellent agreement with the B3LYP/6-311++G(d,p) calculated value of 332 kcal/mol. Hydrogen-bond strengths are known to scale with the gas-phase acidity of the H donor. Note, however, that in solution the N3−H group is more acidic.[49,50]

The S_1 excited-state structures were fully optimized with the CIS method and the 6-31G(d,p) basis set. All three isomers of 2PY·U, 2PY·T, and 2PY·5-FU are slightly pyramidal at the N−H group of the 2-pyridone moiety.[30,31] This has also been observed experimentally for the 2-pyridone monomer.[51] The energy barriers to planarity are very small, in the range 0.025−0.051 kcal/mol; see also the last line in Table 1. These barriers are 2−4 times smaller than the calculated S_1 state vibrational zero-point energy of the 2PY out-of-plane pyramidalization vibration; see below. We expect the S_1 state $v = 0$ vibrational wave function to extend symmetrically over both pyramidal forms, leading to a quasi-planar structure.

TABLE 2: S_1 State Inter- and Intramolecular Vibrational Frequencies and Intermolecular Zero-Point Energies (in cm^{-1}) of 2-Pyridone·Uracil, 2-Pyridone·Thymine, and 2-Pyridone·5-Fluorouracil Isomers, Calculated at the CIS/6-31G(d,p) Level

isomer		U1	U2	U3	T1	T2	T3	F1	F2	F3
Intermolecular Vibrations:										
ν_1	buckle β	19.1	19.1	18.5	17.4	18.8	16.6	17.7	19.2	16.9
ν_2	propeller twist θ	43.9	36.6	36.2	41.6	32.9	35.6	41.5	33.5	36.2
ν_3	stagger δ	61.3	63.7	63.5	59.4	62.0	57.6	60.8	69.8	59.4
ν_4	opening ω	77.8	70.9	80.8	69.9	62.0	64.5	70.5	63.1	66.5
ν_5	shear χ	82.0	85.3	71.1	87.9	84.4	84.8	81.4	80.6	80.3
ν_6	stretch σ	128.5	124.6	121.3	126.4	112.3	120.2	128.9	112.7	121.7
$\mathrm{ZPE}_{\mathrm{inter}}$		206.3	200.0	195.7	201.3	189.0	189.6	200.4	189.5	190.5
Intramolecular Vibrations:										
ν_1(2PY)	2PY butterfly def.	90.0	80.0	85.8	79.7	79.6	78.5	90.0	87.6	88.5
ν_1(T)	CH_3 wagging				128.3	118.4	124.2			
ν_2(T)	CH_3 torsion τ				165.4	169.9	170.3			
ν_4(2PY)	2PY/X ip. ring def.	500.5	499.0	497.7	495.1	498.2	497.7	492.7	495.7	496.4
ν_5(2PY)	2PY/X ip. ring def.	566.6	568.4	568.5	507.4	501.7	501.5	506.4	498.9	499.7
ν_6(2PY)	2PY/X ip. ring def.	574.8	574.5	573.0	574.4	573.9	573.4	573.4	572.4	572.1

2.2. Inter- and Intramolecular Vibrations. The six intermolecular harmonic frequencies of 2PY·U, 2PY·T, and 2PY·5-FU calculated at the CIS/6-31G(d,p) levels are given in Table 2. The B3LYP/6-311++G(d,p) and PW91/6-311++G(d,p) ground-state vibrations are available as Supporting Information. The three out-of-plane (oop) intermolecular vibrations lie in the range 20−80 cm^{-1}.

For all isomers of 2PY·U, 2PY·T, and 2PY·5-FU, the lowest-frequency vibration is the "buckle" mode β at 18−19 cm^{-1}. It is followed by the "propeller twist" mode θ around the in-plane long axis of the dimer. The "stagger" mode δ is a slanting motion, typically at ~60 cm^{-1}; see Figure 2. The in-plane vibrational modes are shown in perspective views in Figure 3. The "opening" (ω) mode derives from conrotatory or cogwheel-like in-plane motions. The corresponding disrotatory motion is the "shear" vibration χ. The highest-frequency intermolecular vibration is always the H-bond stretching mode σ.

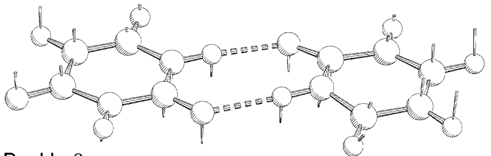
Buckle β
ν_1 = 19.1 cm^{-1}

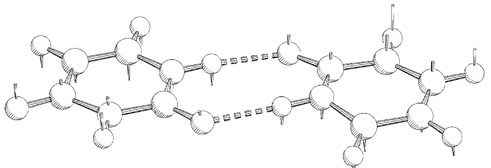
Propeller Twist θ
ν_2 = 43.9 cm^{-1}

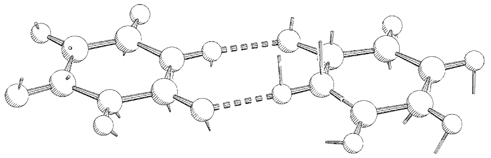
Stagger δ
ν_3 = 61.3 cm^{-1}

Figure 2. CIS/6-31G(d,p) normal modes for the buckle β', propeller twist θ', and stagger δ' vibrations of the U1 isomer of 2-pyridone·uracil.

The lower-lying CIS/6-31G(d,p) S_1 state intramolecular frequencies are also given in Table 2. The lowest-frequency vibration on the 2PY moiety, referred to above as the pyramidalization vibration, lies at 80−90 cm^{-1}, which lies between the intermolecular χ' and σ' vibrations for U1 and a few cm^{-1} lower for T1, between the ω' and χ' vibrations.

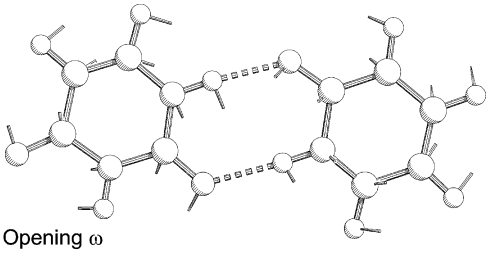
Opening ω
ν_4 = 77.8 cm^{-1}

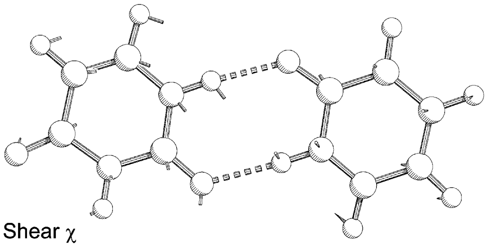
Shear χ
ν_5 = 82.0 cm^{-1}

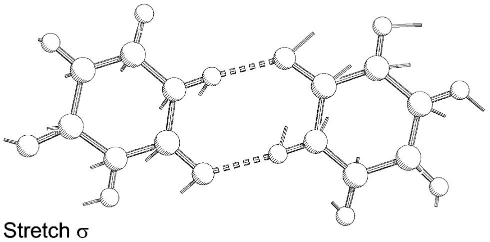
Stretch σ
ν_6 = 128.5 cm^{-1}

Figure 3. CIS/6-31G(d,p) normal modes for the opening ω', shear χ', and stretch σ' intermolecular vibrations of the U1 isomer of 2-pyridone·uracil.

3. Experimental Section

The dimers were synthesized and cooled in 20 Hz pulsed supersonic expansions through a thin-walled 0.6 mm diameter nozzle, using Ne carrier gas at a backing pressure of 2 bar. 2-Pyridone (Aldrich) was placed in a stainless steel container at 95 °C, through which the Ne was flowed to the nozzle via a connection tube held at 105 °C. Uracil, thymine, or 5-fluorouracil (Fluka, 99%) was placed inside the pulsed nozzle, where mixing occurs with the neon/2PY gas stream. The nozzle temperature was 215 °C for experiments on 2PY·U, 185 °C for 2PY·T, and 220 °C for 2PY·5-FU.

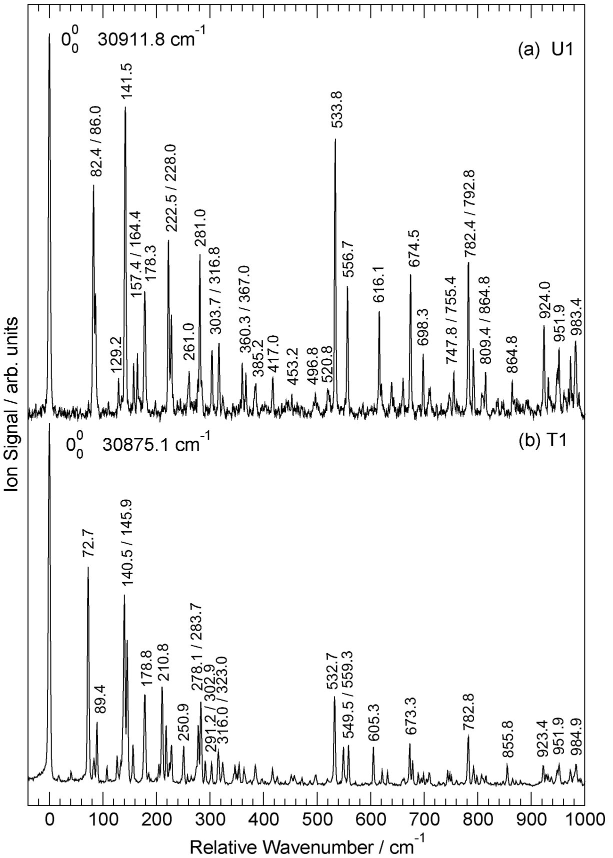

Figure 4. Two-color R2PI spectra of (a) 2-pyridone·uracil and (b) 2-pyridone·thymine. The wavenumber scales are relative to the respective electronic origins at 30 911.6 and 30 874.5 cm^{-1}.

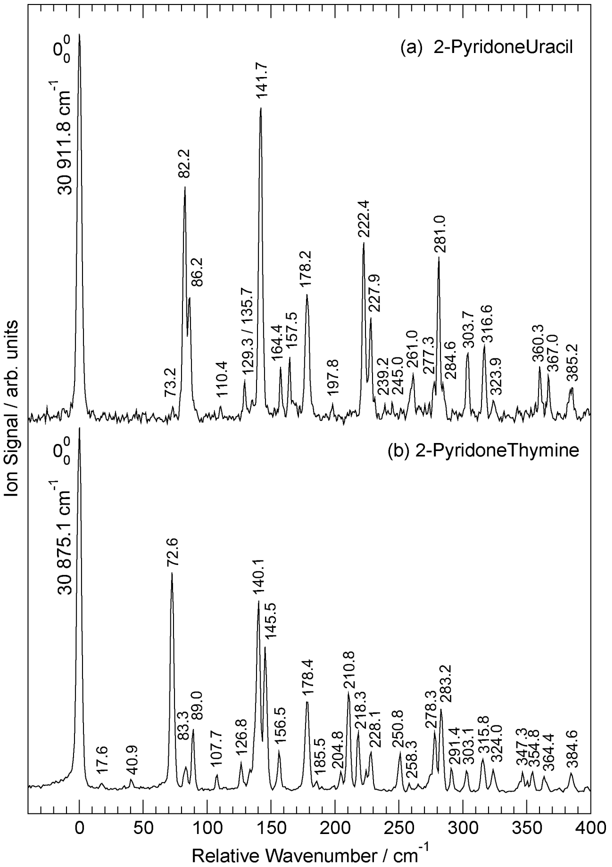

Figure 5. Low-frequency region of the 2C-R2PI spectra of (a) 2-pyridone·uracil and (b) 2-pyridone·thymine. The wavenumber scales are relative to the respective electronic origins.

Mass-selected two-color resonant two-photon ionization (2C-R2PI) spectra were measured by crossing the skimmed supersonic jet with the unfocused UV excitation and ionization lasers, which were brought to spatial and temporal (±0.5 ns) overlap within the source of a linear time-of-flight mass spectrometer. For the $S_1 \leftarrow S_0$ excitation, we employed pulse energies of 0.2−1.0 mJ from a frequency-doubled dye laser pumped by the second harmonic of a Nd:YAG laser. For ionization, the fourth harmonic (266 nm) of the same Nd:YAG laser was used at energies of 1−2 mJ/pulse. To increase the ionization yield, the 266 nm ionization beam was back-reflected through the source of the mass spectrometer. The cluster ions were detected on the expected masses (*m*/*e* 215, 230, and 234, respectively) using double multichannel plates. The time-of-flight mass spectra were digitized in a 1 GS/s transient digitizer (LeCroy LT374), averaged over 64 or 128 laser shots, and transferred to a PC.

For the UV−UV hole-burning experiments, a 1 mJ UV laser pulse depleted the S_0 vibrational ground state, and the residual ground-state population was probed 300 ns later by the R2PI technique on the $S_1 \leftarrow S_0$ electronic origin. Typical depletions were 20−25%. Depletion spectra were recorded either by scanning the UV hole-burning laser or by successive R2PI scans with and without the hole-burning laser. For all three dimers, the UV hole-burning spectra reproduce the 2C-R2PI spectra to ∼1100 cm^{-1}, implying that each spectrum is due to only one species.

4. Results

The $S_1 \leftarrow S_0$ spectra of all three dimers were investigated over the range 30 400−32 000 cm^{-1}. The lowest-frequency bands at 30 911.6 cm^{-1} for 2PY·U, 30 874.5 cm^{-1} for 2PY·T, and 30 978.1 cm^{-1} for 2PY·5-FU are the strongest bands in the spectrum and are assigned as the $S_1 \leftarrow S_0$ origins. They are localized in the 2-pyridone moiety and lie ∼1000 cm^{-1} to the blue of the so-called "A" $S_1 \leftarrow S_0$ origin of 2PY at 29 831.2 cm^{-1}.[29,51,52]

In the gas phase, 2-pyridone also exists in the enol or 2-hydroxypyridine (2HP) form. The gas-phase enol:keto tautomer ratio is 2HP:2PY = 3:1,[53] and the dimers of 2HP with U, T, or 5-FU must also exist in the supersonic beam. However, the $S_1 \leftarrow S_0$ electronic absorption of 2HP lies at ∼35 000 cm^{-1}, 4000 cm^{-1} further to the blue. Thus, we completely discriminate against the dimers with 2HP on spectroscopic grounds.

The orientation of the $S_1 \leftrightarrow S_0$ electronic transition dipole moment of 2-pyridone in the analogous $(2PY)_2$ and 2PY·2HP complexes measured by Pratt and co-workers lies within the plane and roughly perpendicular to the long in-plane axis of the dimer.[29,54] On the basis of the calculated planarity of the S_0 state and near-planarity in the S_1 state and because the $S_1 \leftrightarrow S_0$ electronic transition of 2PY is in-plane, we expect the totally symmetric a′ in-plane vibrations to dominate the vibronic band structure for all three complexes.

4.1. 2-Pyridone·Uracil. An overview 2C-R2PI spectrum of 2PY·U is shown in Figure 4a; Figure 5a shows details of the range 0−400 cm^{-1}. The weak band observed at 45.0 cm^{-1} is assigned to the out-of-plane propeller twist vibration θ', calculated at 43.9 cm^{-1}; see Figure 2. The band at 82.2 cm^{-1} is assigned as the in-plane "opening" fundamental ω', based on its intensity and the CIS calculated frequency $\omega' = 77.8$ cm^{-1}. Consequently, the 86.2 cm^{-1} shoulder on the high-frequency side of the 82.2 cm^{-1} band is assigned to the shear mode χ', in accord with the CIS frequency $\chi' = 82.0$ cm^{-1}; see

TABLE 3: Experimental S_1 State Vibrational Frequencies of 2-Pyridone·Uracil, 2-Pyridone·Thymine, and 2-Pyridone·5-Fluorouracil (in cm^{-1})

2-pyridone·uracil		2-pyridone·thymine		2-pyridone·5-fluorouracil	
0_0^0 ($S_1 \leftarrow S_0$)	30 911.6		30 874.5		30 978.1
		β'	17.6		
θ'	45.0		40.9		
ω'	82.2		72.6		73.5
		$2\theta'$	83.3		
χ'	86.2		89.0		88.0
ν_1'(2PY) or $\theta' + \delta'$	110.4	ν_1'(2PY)	107.7		
$2\delta'$	129.3		126.8		
σ'	141.7		140.1		142.0
		$2\omega'$	145.5		147.6
$\omega' + 2\theta'$	157.5		156.5		156.4
$2\omega'$	164.4				
B	178.2	$B/2\chi'$	178.4	B	177.0
$\omega' + \sigma'$	222.4		210.8		213.7
		$3\omega'$	218.3		221.1
$\chi' + \sigma'$	227.9		228.1		229.2
$3\omega'$	245.0				
$B + \omega'$	258.5		250.8		249.7
$B + \chi'$	261.0		265.5		
$2\sigma'$	281.0		278.3		281.7
$2\omega' + \sigma'$	303.7		283.2		286.3
$B + \sigma'$	316.6				
$4\omega'$	323.9		291.4		294.3
$B + \sigma'$	315.8		315.8		
$B + \omega'$	324.0				
$\omega' + 2\sigma'$	360.3		347.3		359.1
$\chi' + 2\sigma'$	367.0		364.4		367.9
$3\omega' + \sigma'$	385.2		354.8		
$3\sigma'$	417.0		417.2		421.1
$4\omega' + \sigma'$			425.4		
$5\omega' + \sigma'$			497.8		
$\omega' + 3\sigma'$	496.8				
ν_5'(2PY)	533.8		532.7		532.7
$4\sigma'$	556.7		549.5		558.9
ν_5'(2PY) + ω'	616.1		605.3		605.7
ν_5'(2PY) + σ'	674.5		673.3		674.7
ν_{10}'(2PY)	782.4		782.8		782.3
ν_{10}'(2PY) + ω'	856.1				
ν_{13}'(2PY)	924.0		923.4		924.1

Figure 3. The intense vibronic band at 141.7 cm^{-1} is assigned to the hydrogen-bond stretching vibration σ', for which the CIS calculated frequency is $\sigma' = 128.5$ cm^{-1}. The calculated ω' and χ' frequencies are about 5%, the σ' frequency 9% lower than was observed.

Overtone excitations of the opening vibration can be identified up to $4\omega'$ at 323.9 cm^{-1}, and those of the σ' stretch can be identified up to $3\sigma'$ at 417.0 cm^{-1}. Many weak to medium weak bands can be assigned as combinations of ω', χ', and σ'; see Table 3.

The weak band at 129.3 cm^{-1} is too high for an out-of-plane fundamental, while all three in-plane fundamentals are already assigned. We tentatively attribute it to the $2\delta'$ overtone of the "stagger" vibration, which implies a fundamental frequency of $\delta' \approx 64.7$ cm^{-1}. The CIS calculated frequency for δ' is 61.3 cm^{-1}, 5% lower than was observed, similar to those observed for the ω' and χ' fundamentals; see above. The weak band at 110.4 cm^{-1} is assigned as the combination band $\theta' + \delta'$, which is consistent with the previous assignments of θ' and $2\delta'$, from which one predicts 109.7 cm^{-1} for this excitation.

A medium strong band is observed at 178.2 cm^{-1}. Built on this excitation, one finds a number of combination bands with ω', χ', and σ', listed in Table 3. The shear overtone $2\chi'$ is expected at 172 cm^{-1}, but the frequency and the intensity of the observed band are too high for an assignment as $2\chi'$. An out-of-plane ring deformation centered on U is calculated to lie at 181.7 cm^{-1}, but the electronic transition is centered on 2PY, which renders this assignment improbable. We tentatively assign this band in terms of the "B" origin[29,51,52] in bare 2PY: this origin lies 95 cm^{-1} above the A origin and has been interpreted as a conformer origin with pseudoaxial orientation of the N−H bond.[51] One may speculate that this origin is shifted from 95 to 178 cm^{-1} by complexation to uracil. Further supports for this argument are: (i) that this band has a broader rotational contour (3.5 cm^{-1} fwhm) than the other low-lying bands, which have widths of 2.1−2.5 cm^{-1} fwhm. This may reflect a different orientation of the transition dipole moment within the dimer, as would be expected for a pseudoaxial N−H···O=C coordination, which results in a bent dimer. (ii) A medium strong excitation which is difficult to assign is also observed in 2PY·T and 2PY·5-FU, see below, and in the (2-pyridone)$_2$ dimer and its isotopomers at ~191 cm^{-1}. An alternative interpretation of this band is as the first overtone of the 2PY out-of-plane intramolecular pyramidalization deformation mode, $2\nu_1'$(2PY), with a CIS frequency of 90.0 cm^{-1}. It is unclear what the effect of barrier to planarity along the pyramidalization coordinate is on the overtone frequency, but 178 cm^{-1} is not unreasonable.

Summarizing, we note that nearly all of the excitations in the range up to 530 cm^{-1} correspond to the intermolecular in-plane vibrational fundamentals and their overtones and combinations. As expected from the calculations that yielded planar structures for the S_0 and quasi-planar structures for the S_1 state, the out-of-plane excitations are much weaker than the in-plane vibrations.

At 533.8, 782.4, and 924.0 cm^{-1}, intense intramolecular vibrations are observed. These are in-plane ring deformation vibrations of 2PY and are assigned in Table 3. All other bands in the region up to 1000 cm^{-1} are combination bands involving the intermolecular fundamentals discussed above.

4.2. 2-Pyridone·Thymine. The overview and detailed 2C-R2PI spectra of 2PY·T are shown in Figures 4b and 5b. The 0_0^0 transition is at 30 874.5 cm^{-1}, 37.1 cm^{-1} lower than the electronic origin of 2PY·U. Two very weak bands at 17.6 and 40.9 cm^{-1} can be observed, which are assigned as the out-of-plane butterfly β' and propeller twist θ' fundamentals, in excellent agreement with the CIS frequencies $\beta' = 17.4$ cm^{-1} and $\theta' = 41.6$ cm^{-1}. Nontotally symmetric out-of-plane fundamentals are weakly allowed in vibronic spectra of molecular dimers or complexes due to their large-amplitude character.[55] With this amendment, the weakness of these out-of-plane excitations (≤2% of the electronic origin) is consistent with vibronic selection rules for a C_s symmetric system and implies that 2PY·T is either planar or quasiplanar in the S_1 state.

We assign the first strong excitation at 72.6 cm^{-1} to the ω' opening vibration. In contrast to 2PY·U, the χ' shearing mode at 89.0 cm^{-1} is now clearly separated from the ω' excitation. The CIS frequencies are $\omega' = 69.9$ cm^{-1} and $\chi' = 87.9$ cm^{-1}, both slightly lower than observed. The strong band at 140.1 cm^{-1} is assigned to the σ' fundamental, analogous to 2PY·U. As for 2PY·U, overtone progressions are observed for ω' and σ'. Many further combination and overtone bands are listed in Table 3.

The weak band at 126.8 cm^{-1} is assigned to the overtone of the stagger vibration, $2\delta'$, in analogy to 2PY·U. The resulting fundamental frequency $\delta' \approx 63.4$ cm^{-1} is in acceptable agreement with the CIS $\delta' = 59.4$ cm^{-1}. The weak band at 107.7 cm^{-1} is very similar in frequency and intensity to the weak 110.4 cm^{-1} band of 2PY·U. This precludes an assignment as a methyl rotor excitation for 2PY·T. From the above assignments, one would expect the $\theta' + \delta'$ combination band at 104.3 cm^{-1}, in much less good agreement than the 2PY·U

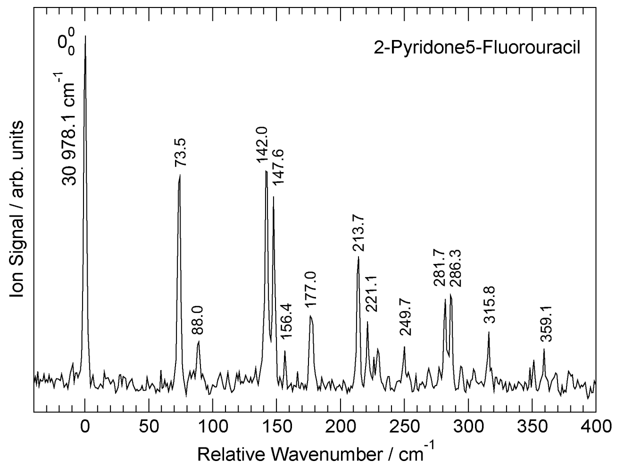

Figure 6. Low-frequency region of the 2C-R2PI spectra of 2-pyridone·5-fluorouracil (2PY·5-FU). The wavenumber scale is relative to the electronic origin.

assignment. An alternative assignment might be as the 2PY out-of-plane pyramidalization mode ν_1', but its calculated 79.7 cm^{-1} frequency is quite far from experiment.

As for 2PY·U, a medium intense band is observed at 178.4 cm^{-1}. Built on this excitation are a number of combination bands involving ω', χ', and σ', as listed in Table 3. As for 2PY·U, the half-width of this band is noticeably larger than that of the other bands. On the basis of the CIS/6-31G(d,p) calculations, it cannot be assigned in terms of an intermolecular vibrational excitation. Again, we tentatively assign it to the analogue of the 2Py B origin.

4.3. 2-Pyridone·5-Fluorouracil. Figure 6 shows the lower 400 cm^{-1} of the two-color R2PI spectrum. The 0^0_0 transition is observed at 30 978.1 cm^{-1}, 66.3 cm^{-1} above the 0^0_0 band of 2PY·U and 103.0 cm^{-1} to the blue of the 2PY·T origin. The overall shape of the spectrum is very similar to those of 2PY·U and 2PY·T. Specifically, the frequencies and Franck−Condon factors of the individual bands are very similar to those of 2PY·T. Most assignments, listed in Table 3, can be made by analogy to the 2PY·T spectrum and are not discussed in detail. It is important that the frequencies ω' and σ' and their combinations and overtones lie at slightly higher frequencies than for 2PY·T, indicating stronger H-bonds.

4.4. Excited-State Lifetimes. The fluorescence lifetime of 2PY has been determined as $\tau_{\mathrm{fl}} = 11 \pm 1$ ns from the width of individually resolved rotational-vibronic lines.[51] Slightly shorter lifetimes $\tau_{\mathrm{fl}} = 9 \pm 1$ ns have been observed for the homodimer $(2PY)_2$[29,30,31] and the complexes 2PY·H_2O, 2PY·$(H_2O)_2$, 2PY·NH_3, and 2PY·$(NH_3)_2$, which are the same within the experimental error at the respective electronic origins.[56,57] The lifetime of 2-aminopyridine·2-pyridone (2AP·2PY) is $\tau_{\mathrm{fl}} = 14 \pm 1$ ns.[58]

By comparison, the fluorescence of 2PY·U, 2PY·T, and 2PY·5-FU is so weak that we have not yet been able to measure either fluorescence lifetimes or spectra. From this, we estimate that the respective fluorescence quantum yields and lifetimes must be <0.05 times those of the aforementioned complexes, and dimers or τ_{fl} must be <500 ps. We also measured the fluorescence lifetimes of 2PY·U and 2PY·T by R2PI excitation/ionization experiments. Given the UV laser pulse widths of 4−5 ns, the 1−2 ns relative trigger jitter, and the use of careful deconvolution techniques, we would have been able to determine fluorescence lifetimes $\tau_{\mathrm{fl}} > 2$ ns, but find no effect due to the excited-state lifetime. These measurements place an independent upper limit of 2 ns on the fluorescence lifetimes of 2PY·U and 2PY·T.

5. Discussion

5.1. Intermolecular Vibrations. *Out-of-Plane Modes*. The R2PI spectra of 2PY·U and 2PY·T exhibit very weak β' and θ' bands, ≤2% of the electronic origins. The symmetry-allowed overtone of the third out-of-plane vibration $2\delta'$ is somewhat more intense than the β' and θ' fundamentals, due to a Fermi resonance with the strong σ' band. Due to the lower signal/noise, we have not observed the out-of-plane vibrations in 2PY·5-FU. For 2PY·U and 2PY·T, the CIS/6-31G(d,p) calculated θ' frequencies are within ~2% of experiment, and the agreement for δ' is also good, within 5−6%. In both cases, methylation at C5 decreases the frequency by the calculated amount.

Opening and Shear Modes. Comparison of the ω' and χ' frequencies of 2PY·U and 2PY·T reveals astonishingly large effects of methylation at C5: ω' decreases by −9.6 cm^{-1} (or −12%) and χ' increases from 86.2 to 89.0 cm^{-1}, by +4%. Methylation at C5 increases the moment of inertia of the uracil moiety around the axis perpendicular to the molecular plane. This should decrease both ω' and χ' frequencies by 5−8%; such decreases are indeed predicted by both B3LYP and PW91 calculations for the S_0 state. Hence, the observed frequency increase of χ' upon methylation cannot be due to the increased moment of inertia. On the other hand, the ω' and χ' frequency changes upon methylation are well reproduced by the CIS/6-31G(d,p) calculations (−7.9 cm^{-1} for ω' and +5.9 cm^{-1} for χ'). Hence, the frequency changes of ω' and χ' must involve changes of the intermolecular force field in the excited electronic state. The $S_1 \leftrightarrow S_0$ transition dipole moment of 2PY is in-plane[29] and approximately perpendicular to the H-bonds. This intramolecular charge flow is expected to influence mainly the ω' and χ' frequencies, because both normal-mode eigenvectors are oriented in the same direction as the dipole moment change.

Stretching Modes and Force Constants. From the σ' frequencies, we calculate the excited-state H-bond stretching force constants $k_{\sigma'}$ in a pseudodiatomic harmonic oscillator model. Modeling the 2PY and uracil molecules as pseudoatoms of mass 95.1 and 112.1 amu each (reduced mass of 51.43 amu) and the intermolecular stretch as a one-dimensional motion, we obtain a stretching force constant $k_{\sigma'} = 60.7$ N/m for 2PY·U. For 2PY·thymine, μ is 54.21 amu, giving $k_{\sigma'} = 63.1$ N/m.

The σ' frequency of 2PY·U decreases by 1.6 cm^{-1} or −1.1% upon C5 methylation. The CIS calculations predict a decrease by −2.1 cm^{-1} (−1.6%) upon methylation; as before, we find the CIS results to be remarkably accurate. If we would assume that the frequency change between 2PY·U and 2PY·T were only due to the increase of the reduced mass, this would decrease the harmonic oscillator frequency by ~3%, a larger frequency decrease than is actually observed! The increase of k_σ by ~4% upon C5 methylation is seen to partially counteract the reduced mass effect on the stretching frequency.

For 2PY·5-FU, $\mu = 54.94$ amu, and the force constant is calculated as $k_{\sigma'} = 65.2$ N/m. The increase of $k_{\sigma'}$ is in agreement with the increase in the calculated binding and dissociation energies; cf. Table 1. For the $(2PY)_2$ homodimer,[30,31] $\sigma' = 153.1$ cm^{-1} is about 9% larger than 2PY·5-FU; due to the smaller reduced mass of $(2PY)_2$, the stretching force constant is nearly the same, $k_{\sigma'} = 65.7$ N/m.

5.2. Intramolecular Out-of-Plane Motions. For the closely related $(2PY)_2$ dimer and its d_1 and d_2 isotopomers, the analysis of the rotationally resolved electronic spectra[51,29] has shown that this dimer is planar in the S_2 excited state (the S_1 state lies closely below, but cannot be observed for the d_0 and d_2 species due to selection rules).[29,30] The rotationally resolved electronic spectrum of the closely related dimer 2-pyridone·2-hydroxypyridine has also been interpreted in terms of a planar S_1 state structure.[54] On the other hand, the 2PY monomer is slightly nonplanar in its S_1 state and exhibits two origins A and B, assigned to two separate invertamers.[51]

We have interpreted the 2C-R2PI spectra of 2PY•U, 2PY•T, and 2PY•5-FU also in terms of planar S_1 state structures. On the other hand, the propensity of the 2PY chromophore to excited-state pyramidalization at the N atom is apparent from the weak transitions at 108−110 cm^{-1} and the medium strong bands at 177−178 cm^{-1} which appear for all three dimers. We cannot assign these transitions in terms of intermolecular fundamentals, overtones, or combinations and attribute them to intramolecular out-of-plane vibrations of 2PY. The CIS calculation predicts an out-of-plane ring deformation vibration localized on 2PY at 90.0 cm^{-1}; the $v' = 2$ level of this is expected to lie at ~180 cm^{-1}, and we tentatively assign the 178.2 cm^{-1} medium strong band to such a transition. A related assignment would be as the analogue of the B origin of 2PY that is shifted from +95 cm^{-1} in 2PY to +180 cm^{-1} in the 2PY•U, 2PY•T, and 2PY•5-FU complexes.

The CIS calculations also predict an out-of-plane ring deformation vibration localized on the U (and T) moieties at 181.7 cm^{-1} (184.3 cm^{-1}), respectively. However, the electronic transition is localized on the 2PY moiety, and because we do not observe strong out-of-plane fundamentals on 2PY, we expect even less activity on U (or T).

5.3. Excited-State Lifetimes and Fluorescence Quenching in 2PY·U and 2PY·T. As discussed above, the fluorescence of 2PY•U, 2PY•T, and 2PY•5FU is ~20 times weaker than that of the other 2PY•X complexes measured so far. This could be due to changes of intramolecular nonradiative processes of 2PY induced by the H-bonding to U and T. Conceivable mechanisms are as follows:

(i) Increase of internal conversion (IC) rate of 2PY. However, the near-constancy of the observed fluorescence lifetimes of all other 2PY•X complexes involving single and double H-bonds of widely different strengths (see above) implies that IC in 2PY is not very susceptible to the number of hydrogen bonds or the H-bond strength, arguing against this mechanism. Also, the efficiency of IC usually increases rapidly with excess vibrational energy in the S_1 state, leading to the disappearance of the vibronic structure in the spectrum. This is in strong contrast to the observed R2PI spectra that extend up to 1500 cm^{-1} above the origin.

(ii) Increase of intersystem crossing (sensitized ISC) within the 2PY molecule. This process is mediated by heavy atoms that contribute sufficiently large spin−orbit coupling matrix elements (external heavy atom effect). Neither U, T, nor 5-FU contains any such atoms, refuting this mechanism.

(iii) Intermolecular singlet−triplet transfer: This is a highly spin-forbidden process.[63] It has only been conclusively observed for quenchers containing heavy atoms (Br) with low-lying triplet T_1 states. The T_1 and T_2 states of uracil are lower than the S_1 state of 2PY,[40] but the absence of heavy atoms in uracil and thymine also argues against this mechanism.

(iv) Intermolecular singlet−singlet electronic energy transfer from 2PY to U, T, or 5-FU as acceptor. This can occur in 2PY•X complexes if the S_1 state of X lies below that of 2PY. For X = H_2O, NH_3, and the corresponding $n = 2$ clusters, the S_1 electronic states are higher than the S_1 state of 2PY. For X = 2-hydroxypyridine and 2-aminopyridine, the $S_1 \leftarrow S_0$ excitations in the gas phase are experimentally known to lie at 36 136[52] and 33 471 cm^{-1},[59] 2500−5000 cm^{-1} higher than the excitation energy used here. All of these complexes exhibit ~10 ns lifetimes.

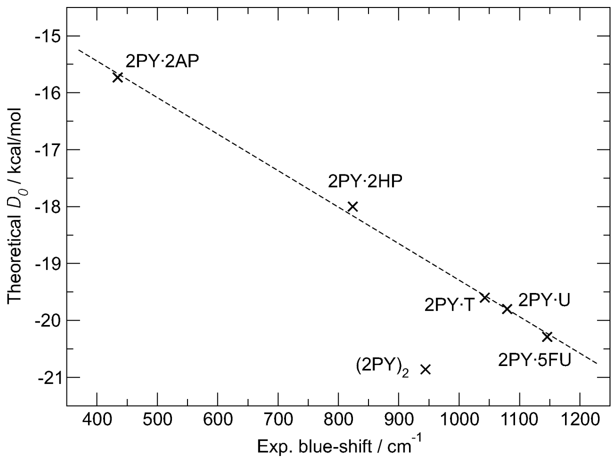

Figure 7. Experimental spectral blue-shifts $\delta\nu$ of the doubly H-bonded dimers 2-pyridone•X (X = 2-aminopyridine, 2-hydroxypyridine, 2-pyridone, uracil, thymine, 5-fluorouracil), relative to the A 0_0^0 band of 2PY, plotted versus the respective PW91/6-311++G(d,p) dissociation energies D_0.

The gas-phase R2PI spectra of U and T show onsets slightly below 36 600 and 36 300 cm^{-1}, respectively.[25] Recent ab initio studies have shown that these are the $S_2 \leftarrow S_0$ transitions, to the lowest $\pi\pi^*$ state.[35,40] The S_1 state is an $n\pi^*$ state with near-zero oscillator strength from the S_0 state. Recent work using DFT/multireference configuration interaction (MRCI) methods[40] places the $n\pi^*$ state minimum of uracil at 3.95 eV or 31 900 cm^{-1}, only ~1000 cm^{-1} (0.12 eV) above the electronic origins of 2PY•U, 2PY•T, and 2PY•5-FU, and within the typical deviation of the DFT/MRCI method (0.15 eV RMS for 37 different aromatic molecules).[60] Thus, the S_1 $n\pi^*$ state of uracil may lie at the same energy or even slightly below that of 2PY. The singlet−singlet energy transfer rate for 2PY ↔ 2PY in the same H-bond geometry is known from the exciton splitting between the S_1/S_2 states of $(2PY)_2$ to be 3×10^{12} s^{-1}.[31] The singlet−singlet transfer in 2PY•U and 2PY•T is much slower, because the oscillator strength of the uracil $S_1 \leftarrow S_0$ $n\pi^*$ transition is calculated[40] to be only $f = 2 \times 10^{-4}$. In addition, there are considerable geometry changes between the uracil S_0 and S_1 states, see Figures 2 and 6 in ref 40, leading to low Franck−Condon factors for this transition. The same situation probably prevails for T and 5-FU. If we assume a singlet−singlet transfer rate of only $k_{\mathrm{transf}} = 3 \times 10^9$ s^{-1} from 2PY to U, T, and 5-FU, this would explain the near-complete absence of fluorescence from 2PY in the title complexes.

5.4. Electronic Spectral Shifts. The $S_1 \leftrightarrow S_0$ electronic origins of 2PY•U, 2PY•T, and 2PY•5-FU are shifted to the blue of the A origin of 2PY by $\delta\nu = D_0(S_1) - D_0(S_0) = 1050$−1150 cm^{-1}. Electronic excitation lowers the S_1 state dissociation energy by 3.0−3.3 kcal/mol, which is 15% of the PW91 S_0 state dissociation energy $D_0(S_0)$. Blue-shifts have also been observed for other doubly H-bonded complexes of 2PY, for example, $(2PY)_2$,[28−31] 2PY•2-hydroxypyridine,[54,61] and 2PY•2-aminopyridine.[58] In Figure 7, we plot the PW91 calculated dissociation energies $D_0(S_0)$ versus the experimental spectral blue-shifts $\delta\nu$. With the exception of the $(2PY)_2$ dimer, which exhibits exciton splittings of its S_1/S_2 states, the spectral shift scales nearly linearly with $D_0(S_0)$. According to this plot, $\delta\nu$ extrapolates to zero at $D_0(S_0) = 12.9 \pm 0.1$ kcal/mol. This implies that the observed decrease of dissociation energy upon electronic excitation is a nearly constant fraction of a part of the ground-state binding energy.

In hydrogen-bonding solvents, $\pi\pi^*$ transitions typically shift to lower frequency upon H-bond formation, while nπ^* transitions shift to the blue.[62] Large blue-shifts upon solvation are also typical for Rydberg transitions, due to repulsion of the large Rydberg orbitals by the surrounding solvent. The $S_1 \leftrightarrow S_0$ transition of 2PY is a $\pi\pi^*$ transition by all experimental criteria, that is, in-plane transition dipole moment, large high oscillator strength, and short excited-state lifetimes.[29,30,56,57] While the spectral blue-shifts might be due to mixing of a low-lying nπ^* state with the $\pi\pi^*$ S_1 state, we consider the mixing with a Rydberg-type $\pi\sigma^*$ state to be more probable. The important role of $\pi\pi^*/\pi\sigma^*$ state crossings for the excited-state photophysics of phenol has been investigated by Sobolewski and Domcke,[63,64] and the implications for the photochemistry of aromatic molecules, especially excited-state hydrogen transfer, have also been discussed.[65,66]

6. Conclusions

2PY·U, 2PY·T, and 2PY·5-FU are model systems for the (uracil)$_2$, uracil·thymine, and uracil·5-fluorouracil nucleic acid base pairs that occur in natural or synthetic RNA. These model dimers are accessible to vibronic R2PI spectroscopy, because 2PY is sufficiently long-lived in the S_1 excited state, whereas the uracil, thymine, or 5-fluorouracil bases have extremely short excited-state lifetimes. However, the near-absence of fluorescence from 2PY·U, 2PY·T, and 2PY·5-FU implies that the S_1 state lifetime of the 2PY chromophore in these complexes is $\leq$500 ps, ~20 times less than for all other 2PY·X complexes measured so far. We suggest singlet−singlet energy transfer from 2PY to the nπ^* S_1 states of uracil, thymine, and 5-fluorouracil as the cause. Recent high-level calculations[40] predict these to lie at approximately the required energy and to have very low oscillator strengths from the respective S_0 states, which explains why they have so far not been observed.

UV hole-burning measurements show that for all three dimers only one species is observed in the range from the electronic origins to ~1100 cm^{-1} above. On the basis of PW91 DFT calculations, we attribute these to the doubly N−H···O═C isomers linked via the N1−H and C2═O functional groups of U, T, and 5-FU, denoted U1, T1, and F1. Under biological conditions, the N1−H functional groups of the pyrimidine nucleobases are glycosylated, so the U1, T1, and F1 dimers are not those observed in RNAs. These "sugar-edge" isomers are about 4 and 5 kcal/mol more stable than the two Watson−Crick isomers, which are of similar H-bond strength and are denoted U2/U3, T2/T3, and F2/F3, respectively. We are currently investigating the Watson−Crick dimers, which do form in the supersonic jet when the N1−H position of uracil or thymine is chemically blocked.

In the S_1 state, the three in-plane H-bond vibrations, ω', χ', σ', and the overtone of the stagger mode $2\delta'$ were measured for all three dimers. In addition, weak out-of-plane buckle β' and propeller twist τ' fundamentals were observed for 2PY·U and 2PY·T. The observed frequencies are 1−5 times higher than the harmonic frequencies calculated by the CIS/6-31G(d,p) method for the U1, T1, and F1 isomers, respectively. These CIS calculations reliably predict the frequency splittings between the ω' and χ' modes, which are highly specific for the different isomers U1/U2/U3 and T1/T2/T3, as well as the frequency decreases and increases that occur upon methylation and fluorination at the C5 position of uracil.

Relative to 2PY·U, methylation at C5 leads to an increase in the measured H-bond stretching force constant of 4%. However, the calculated dissociation energy is approximately the same. Fluorination at C5 leads to an increase of the stretching force constant by 7.4% and an increase of D_0 by 2.5%.

Acknowledgment. This work was supported by the Schweiz. Nationalfonds (proj. no. 2000-68081.02) and by the Centro Svizzero di Calcolo Scientifico (CSCS) in Manno, Switzerland.

Supporting Information Available: Table of the B3LYP/6-311++G(d,p) and PW91/6-311++G(d,p) ground-state vibrations. This material is available free of charge via the Internet at http://pubs.acs.org.

References and Notes

(1) Chen, Y. Z.; Prohofsky, E. W. *J. Chem. Phys.* **1984**, *80*, 6291.
(2) Chen, Y. Z.; Prohofsky, E. W. *J. Chem. Phys.* **1991**, *94*, 4665.
(3) Cocco, S.; Monasson, R. *J. Chem. Phys.* **2000**, *112*, 10017.
(4) Urabe, H.; Hayashi, H.; Tominaga, Y.; Nishimura, Y.; Kubota, K.; Tsuboi, M. *J. Chem. Phys.* **1985**, *82*, 531.
(5) Urabe, H.; Sugawara, Y.; Tsukakoshi, M.; Kasuya, T. *J. Chem. Phys.* **1991**, *95*, 5519.
(6) Nir, E.; Brauer, B.; Grace, L.; de Vries, M. S. *J. Am. Chem. Soc.* **1999**, *121*, 4896.
(7) Nir, E.; Imhof, P.; Kleinermanns, K.; de Vries, M. S. *J. Am. Chem. Soc.* **2000**, *122*, 8091.
(8) Nir, E.; Imhof, P.; Kleinermanns, K.; de Vries, M. S. *Nature (London)* **2000**, *408*, 949.
(9) Nir, E.; Janzen, C.; Imhof, P.; Kleinermanns, K.; de Vries, M. S. *J. Chem. Phys.* **2001**, *115*, 4604.
(10) Plützer, C.; Nir, E.; de Vries, M. S.; Kleinermanns, K. *Phys. Chem. Chem. Phys.* **2001**, *3*, 5466.
(11) Nir, E.; Janzen, C.; Imhof, P.; Kleinermanns, K.; de Vries, M. S. *Phys. Chem. Chem. Phys.* **2002**, *4*, 740.
(12) Nir, E.; Janzen, C.; Imhof, P.; Kleinermanns, K.; de Vries, M. S. *Phys. Chem. Chem. Phys.* **2002**, *4*, 732.
(13) Nir, E.; Müller, M.; Grace, L. I.; de Vries, M. S. *Chem. Phys. Lett.* **2002**, *355*, 59.
(14) Plützer, C.; Hünig, I.; Kleinermanns, K.; Nir, E.; de Vries, M. *Chem. Phys. Chem.* **2003**, *4*, 838.
(15) Kim, N. J.; Jeong, G.; Kim, Y. S.; Sung, J.; Kim, S. K.; Park, Y. D. *J. Chem. Phys.* **2000**, *113*, 10051.
(16) Lührs, D.; Viallon, J.; Fischer, I. *Proc. Natl. Acad. Sci. U.S.A.* **2001**, *3*, 1827.
(17) Cech, T. R.; Damberger, S. H.; Gutell, R. R. *Nat. Struct. Biol.* **1994**, *1*, 273.
(18) Grüene, M.; Fürste, J. P.; Klussmann, S.; Erdmann, V. A.; Brown, L. R. *Nucleic Acids Res.* **1996**, *24*, 2592.
(19) Wahl, M. C.; Rao, S. T.; Sundaralingam, M. *Nat. Struct. Biol.* **1996**, *3*, 24.
(20) Lietzke, S. E.; Barnes, C. L.; Berglund, J. A.; Kundrot, C. E. *Structure* **1996**, *4*, 917.
(21) Cate, J. H.; Gooding, A. R.; Podell, E.; Zhou, K.; Golden, B. L.; Kundrot, C. E.; Cech, T. R.; Doudna, J. A. *Science* **1996**, *273*, 1678.
(22) Ban, N.; Nissen, P.; Hansen, J.; Moore, P. B.; Steitz, T. A. *Science* **2000**, *289*, 905.
(23) Matthews, D. A.; Villafranca, J. E.; Janson, C. A.; Smith, W. W.; Welsh, K.; Freer, S. *J. Mol. Biol.* **1990**, *214*, 937.
(24) Voet, D.; Voet, J. G. *Biochemistry*; J. Wiley: New York, 1995.
(25) Brady, B. B.; Peteanu, L. A.; Levy, D. H. *Chem. Phys. Lett.* **1988**, *147*, 538.
(26) Onidas, D.; Markovitsi, D.; Marguet, S.; Sharonov, A.; Gustavsson, T. *J. Phys. Chem. B* **2002**, *106*, 11367.
(27) Gustavsson, T.; Sharonov, A.; Markovitsi, D. *Chem. Phys. Lett.* **2002**, *351*, 195.
(28) Held, A.; Pratt, D. *J. Am. Chem. Soc.* **1990**, *112*, 8629.
(29) Held, A.; Pratt, D. *J. Chem. Phys.* **1992**, *96*, 4869.
(30) Müller, A.; Talbot, F.; Leutwyler, S. *J. Chem. Phys.* **2000**, *112*, 3717.
(31) Müller, A.; Talbot, F.; Leutwyler, S. *J. Chem. Phys.* **2002**, *116*, 2836.
(32) Müller, A.; Losada, M.; Leutwyler, S. *J. Phys. Chem. A* **2004**, *108*, 157.
(33) Kratochvil, M.; Engkvist, O.; Sponer, J.; Jungwirth, P.; Hobza, P. *J. Phys. Chem. A* **1998**, *102*, 6921.
(34) Scanlan, M. J.; Hillier, I. H. *J. Am. Chem. Soc.* **1984**, *106*, 3737.
(35) Lorentzon, J.; Fülscher, M. P.; Roos, B. O. *J. Am. Chem. Soc.* **1995**, *117*, 9265.
(36) Tian, S. X.; Zhang, C. F.; Zhang, Z. J.; Chen, X. J.; Xu, K. Z. *Chem. Phys.* **1999**, *242*, 217.

(37) Wolken, J. K.; Tureček, F. *J. Am. Soc. Mass Spectrom*. **2000**, *11*, 1065.

(38) Kryachko, E. S.; Nguyen, M. T.; Zeegers-Huyskens, T. *J. Phys. Chem. A* **2001**, *105*, 1288.

(39) Shukla, M. K.; Leszczynski, J. *J. Phys. Chem. A* **2002**, *106*, 8642.

(40) Marian, C. M.; Schneider, F.; Kleinschmidt, M.; Tatchen, J. *Eur. Phys. J. D* **2002**, *20*, 357.

(41) Boys, S. F.; Bernardi, F. *Mol. Phys*. **1970**, *19*, 553.

(42) Valiron, P.; Mayer, I. *Chem. Phys. Lett*. **1997**, *275*, 46.

(43) Bukowski, R.; Jeziorski, B.; Szalewicz, K. *J. Chem. Phys*. **1996**, *104*, 3306.

(44) Losada, M.; Müller, A.; Leutwyler, S., to be submitted.

(45) Leininger, M. L.; Nielsen, I. M. B.; Colvin, M. E.; Janssen, C. L. *J. Phys. Chem. A* **2002**, *106*, 3850.

(46) Leontis, N. B.; Stombaugh, J.; Westhof, E. *Nucleic Acids Res*. **2002**, *30*, 3479.

(47) Nguyen, M.; Chandra, K.; Zeegers-Huyskens, T. *J. Chem. Soc., Faraday Trans*. **1998**, *94*, 1277.

(48) Chandra, A. K.; Nguyen, M. T.; Zeegers-Huyskens, T. *J. Phys. Chem. A* **1998**, *102*, 6010.

(49) Kurinovich, M. A.; Lee, J. K. *J. Am. Chem. Soc*. **2000**, *122*, 6258.

(50) Jang, Y. H.; Sowers, L. C.; Çağin, T.; Goddard, W. A., III. *J. Phys. Chem. A* **2001**, *105*, 274.

(51) Held, A.; Champagne, B. B.; Pratt, D. *J. Chem. Phys*. **1991**, *95*, 8732.

(52) Coussan, S.; Manca, C.; Tanner, C.; Bach, A.; Leutwyler, S. *J. Chem. Phys*. **2003**, *119*, 3774.

(53) Nimlos, M. R.; Kelley, D. F.; Bernstein, E. R. *J. Phys. Chem*. **1989**, *93*, 643.

(54) Hatherley, L. D.; Brown, R. D.; Godfrey, P. D.; Pierlot, A. P.; Caminati, W.; Damiani, D.; Melandri, S.; Favero, L. B. G. *J. Phys. Chem*. **1993**, *97*, 46.

(55) Borst, D. R.; Roscioli, J. R.; Pratt, D. W.; Florio, G. M.; Zwier, T. S.; Müller, A.; Leutwyler, S. *Chem. Phys*. **2002**, *283*, 341.

(56) Maxton, P. M.; Schaeffer, M. W.; Ohline, S. M.; Kim, W.; Venturo, V.; Felker, P. M. *J. Chem. Phys*. **1994**, *101*, 8391.

(57) Held, A.; Pratt, D. *J. Am. Chem. Soc*. **1993**, *115*, 9708.

(58) Held, A.; Pratt, D. *J. Am. Chem. Soc*. **1993**, *115*, 9718.

(59) Müller, A.; Talbot, F.; Leutwyler, S. *J. Am. Chem. Soc*. **2002**, *124*, 14486.

(60) Hager, J.; Wallace, S. *J. Phys. Chem*. **1985**, *89*, 3833−3841.

(61) Grimme, S.; Waletzke, M. *J. Chem. Phys*. **1999**, *111*, 5645.

(62) Müller, A.; Talbot, F.; Leutwyler, S. *J. Chem. Phys*. **2001**, *115*, 5192.

(63) Turro, N. J. *Modern Molecular Photochemistry*; Benjamin: Menlo Park, 1978.

(64) Sobolewski, A. L.; Domcke, W. *Phys. Chem. Chem. Phys*. **1999**, *1*, 3065.

(65) Sobolewski, A. L.; Domcke, W. *J. Phys. Chem. A* **2001**, *105*, 9275.

(66) Sobolewski, A. L.; Domcke, W.; Dedonder-Lardeux, C.; Jouvet, C. *Phys. Chem. Chem. Phys*. **2002**, *4*, 1093.